FUDMA Journal of Sciences (FJS)
ISSN online: 2616-1370
ISSN print: 2645 - 2944
Vol. 9 No. 12, December (Special Issue), 2025, pp 675 – 684
DOI: https://doi.org/10.33003/fjs-2025-0912-4287

AN INVESTIGATION ON THE IMPACT OF TEMPERATURE AND THICKNESS VARIATION ON THE PERFORMANCE OF $CuAlO_2$/ZnO AND NiO/ZnO PEROVSKITE SOLAR CELL: A NUMERICAL SIMULATION APPROACH

***[1]Mohammad Aminu Tukur, [2]Darma Tijjani Hassan, [1]Aujara Kabiru Musa**

[1]Department of Science laboratory Technology, Jigawa State Polytechnic, Dutse, Jigawa State, Nigeria.
[2]Department of Physics, Bayero University, KanoState, Nigeria.
[3]Department Statistics, Jigawa State Polytechnic, Dutse, Jigawa State, Nigeria.

*Corresponding authors' email: matukur@jigpoly.edu.ng

ABSTRACT

This study presents a numerical simulation of CuAlO2/ZnO, and NiO/ZnO perovskite solar cells (PSCs) using SCAPS-1D software focussing on the impact of temperature variation (300-400K) and layer thickness optimization (50-140nm, varied in 10nm intervals) on device performance. The investigation evaluates key photovoltaic parameters including open circuit voltage (Voc), short circuit current (Jsc), fill factor (FF), and power conversion efficiency (PCE) to determine the optimal design configurations for improved efficiency. The result reveals that, for the CuAlO2/ZnO, increasing the operating temperature leads to a gradual decline in Voc, from 1.05 to 0.91V, while Jsc increased slightly from 23.1mA/cm2 to 25.4mA/cm2. However, FF dropped from 78% to 68% and PCE declined from 18% at 300K to 13.5% at 400K due to enhanced carrier recombination and decreased built in potential. The device optimal performance was obtained at a CuAlO2 thickness of 90nm and ZnO thickness of 100nm achieving Voc=1.05V, Jsc=23.8mA/cm2, FF=78% and PCE=18.6%. In contrast, for the NiO/ZnO configuration Voc reduces from 1.02V at 300K to 0.89V at 400K, while Jsc slightly increased from 24.3mA/cm2 to 26.1mA/cm2 and FF fell from 76% to 66% leading to PCE drop from 18.9% to 14.2%. Layer thickness strongly influences light absorption and charge transport. The NiO/ZnO device showed its optimum performance with a NiO and ZnO layer thicknesses of 100 and 110nm respectively, producing Voc=1.02V, Jsc=24.3mA/cm2, FF=76% and PCE=18.9%. These findings highlight that precise optimization of HTL and ETL thicknesses withing the 50-140nm range significantly enhances light absorption and charge extraction, while careful control of operating temperature is critical to minimize thermal loses. This work provides valuable insights into the design and optimization of high efficiency thermally stable perovskite solar cells.

Keywords: SCAPS-1D CuAlO2/ZnO, NiO, HTL, ETL, VOC, Jsc, PCE, Photovoltaic perovskite solar cells, temperature variation, layer thickness(50=140nm)

INTRODUCTION

Perovskite solar cells (PSCs) have emerged as promising next-generation photovoltaic devices due to their exceptional power conversion efficiencies (PCEs), tunable bandgaps, low fabrication costs, and compatibility with flexible substrates (Mahmood, *et al*., 2017). Their ABX3 crystal structure allows for strong light absorption, high carrier mobility, and adjustable optoelectronic properties, making them highly suitable for both single-junction and tandem configurations (Bouich, *et al*., 2023). However, PSC performance is strongly influenced by transport layers specifically the hole transport layer (HTL) and electron transport layer (ETL). Optimization of these layers is critical to improving charge extraction, minimizing recombination losses, and enhancing long-term device stability (Sarkar, *et al*., 2024). Copper (I) Aluminum Oxide ($CuAlO_2$) as a hole transport layer is p-type delafossite oxide with a wide bandgap (~3.5 eV), its thickness sets the trade off between sheet resistance/ohmic contact and optical transmission/series resistance. (Bouich *et al*., 2023). Experimental PCS work using $CuAlO_2$ typically employs tens to~160nm-scale films, for example Savva, *et al*., (2019). Used a treated $CuAlO_2$/Cu-O HTL with an average thickness of ≈50nm in inverted PSCs and reported interfacial recombination and stable performance, indicating that very thin, well covered films can work when morphology is well controlled. Reviews on p-type TCOs and inorganic HTLs underscores that going too thin (<50nm) risks incomplete coverage and shunt pathways while going too thick (>150nm) introduces parasitic absorption and series-resistance penalties that lower FF and PCE so a practical sweet spot for compact HTLs sits around 80-120nm stack dependent (Fleischer, 2017).

Across p-i-n perovskite solar cells, the best-performing NiO_x HTLs are usually in the thickness range of 60-120nm which balances full surface coverage against added series resistance and optical loss at lager thicknesses. Islam *et al*., (2017) found 90±5nm gave the optimum thickness performance in solution-processed inverted cells while thinner or thicker films underperformed due to coverage and transport penalties. Likewise, Wang *et al*., (2018) reported an optimal NiO_x performance thickness ≈120nm consistent with transport/optical trade-offs observed experimentally. Also Studies using oxidized Ni films (converted to NiO_x) commonly employed~100nm precursors reflecting the need for robust coverage without excessive resistance (Abdoulsaad, 2019).

The thickness of ZnO electron transport layer (ETL) plays a vital role in balancing optical transparency and charge transport in perovskite solar cells. Several studies have consistently shown that very thin ZnO layers (<50-60nm) often suffer from incomplete coverage and shunting paths while excessive thick layers (>150nm) increase series resistance and hinders charge extraction efficiency (Mohammadian *et al*., 2018). Also, Hossein *et al*., (2023) reported that the optimal ETL thicknesses typically falls between 50 and 100nm across different device stacks, with higher performance observed within this range due to balance of low resistance and minimal optical loss. Similarly,

Gulomova *et al*., (2024) identified ~ 100nm as the optimum ZnO thickness for inverted perovskite devices, noting a significant decline in fill factor and PCE when thickness exceeded ~ 120nm.

Temperature is a crucial factor influencing PSC performance and stability. According to the Shockley–Queisser limit, higher temperatures increase intrinsic carrier concentration, raising the saturation current density (Jsc) and thus lowering open-circuit voltage (Voc), FF, and PCE (Shockley, and Queisser, 1961). Dupré and Green (2015) demonstrated that elevated temperatures also accelerate phonon scattering and defect-assisted recombination, leading to significant performance degradation. Additionally, temperature-induced ion migration and phase instability in hybrid perovskites contribute to device hysteresis and long-term instability (Tumen, *et al*., 2020). Thus, understanding temperature-dependent behaviors is essential for optimizing device operation under real-world conditions. The effects of thickness and temperature are interdependent. Optimized transport-layer thickness can reduce temperature, induced recombination losses by improving band alignment and suppressing defect-mediated trap states (Wu *et al*., 2022). Conversely, non-optimized thicknesses exacerbate thermal degradation, accelerating performance decay at elevated temperatures. For example, Sarkar *et al*., (2024) reported that optimized $CuAlO_2$ HTLs significantly improve device thermal stability up to 360K. Similarly, Mann *et al*., (2024) found that interface-engineered NiO layers mitigate temperature-driven non-radiative losses, maintaining higher PCE under operational stress. These findings underscore the importance of jointly optimizing transport-layer thicknesses and thermal tolerance to design high performance, stable PSCs.

SCAPS-1D (Solar Cell Capacitance Simulator), developed at Ghent University, is a powerful tool for modelling thin-film solar cells under varying physical and operational parameters (Burgelman, *et al*., 2000). It allows for precise simulation of Layer thickness optimization, Interface defect dynamics, temperature-dependent recombination mechanisms and variations in FF, and PCE. Previous studies have validated SCAPS as an effective platform for predicting PSC performance trends and guiding experimental fabrication. This makes it a suitable choice for investigating the combined effects of thickness and temperature variations in $CuAlO_2$/ZnO and NiO/ZnO perovskite solar cells. Despite extensive studies on PSC performance, few works have simultaneously examined the coupled influence of temperature and transport-layer thickness in $CuAlO_2$/ZnO and NiO/ZnO architectures. Existing literature primarily optimizes either temperature tolerance or layer thickness independently, leaving a gap in understanding their combined effects on photovoltaic efficiency and stability. This research addresses this gap by performing a numerical simulation to analyze how temperature variations (300–400 K) and transport-layer thicknesses (50–140nm) jointly affect FF, and PCE. In this work, SCAPS-1D was employed to numerically investigate the coupled effects of temperature variation (300 K–400 K) and transport-layer thicknesses (50–140nm) on the performance of $CuAlO_2$/ZnO and NiO/ZnO perovskite solar cells. The study evaluates key photovoltaic parameters, including I-V characteristics, short-circuit current density (Jsc), open-circuit voltage (Voc), fill factor (FF), and power conversion efficiency (PCE). The results provide insight into optimal device architectures and operating conditions, serving as a guideline for experimental fabrication and large-scale deployment of high performance PSCs.

Theoretical Framework

Perovskite solar cells (PSCs) have emerged as a promising photovoltaic technology due to their exceptional power conversion efficiencies (PCEs) and the potential for low-cost production (Kojima *et al*., 2009; Green *et al*., 2022). To achieve high performance and stability, the design and optimization of charge transport layers (CTLs) are crucial. Metal oxide-based materials such as $CuAlO_2$ and NiO, when combined with ZnO, are particularly attractive for use in PSCs due to their favourable energy band alignment, high hole mobility and good chemical and thermal stability (Ahn *et al*., 2015; Navas *et al*., 2018). The performance of PSCs is highly dependent on key parameters including temperature, layer thickness, and the electrical properties of each functional layer. Temperature variations influence charge carrier dynamics by affecting carrier mobility, recombination rates, and the intrinsic bandgap of the perovskite absorber (Chowdhury *et al*., 2020). Similarly, the thickness of the absorber and transport layers determines light absorption efficiency and charge extraction balance; excessively thick layers can induce recombination losses, while layers that are too thin may cause incomplete light harvesting (Tress, 2017). Electrical properties such as carrier concentration, defect density, and mobility in the transport layers also critically affect device performance by modulating the built-in electric field and minimizing recombination losses (You *et al*., 2016). Numerical simulation tools, such as SCAPS-1D and wxAMPS, have been widely used to investigate these parameters systematically, allowing for the prediction of device behaviour and optimization of layer configurations (Burgelman *et al*., 2000; Abdelrazek *et al*., 2021).Therefore, by applying numerical simulation to study $CuAlO_2$/ZnO and NiO/ZnO-based PSCs, it becomes possible to gain insights into how variations in temperature and layer thickness, influence electric performance metrics such as open-circuit voltage, short-circuit current density, and fill factor, ultimately guiding experimental optimization for high-efficiency devices. A solar cell converts light energy into electrical energy, and its behaviour can be represented using an equivalent circuit model of fig.1 below, it includes current source, diodes, series resistance and a shunt resistance. The equation governing the output current (I) of the solar cell for two diodes of the equivalent circuit is given in equation 1 below

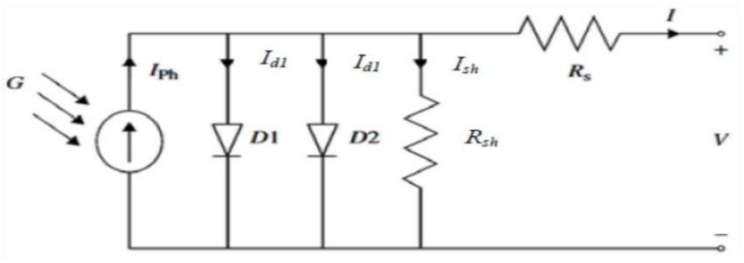

Figure 1: Equivalent Circuit of a Solar cell (El-Ahmar, 2016)

$$I=I_{ph}-I_{D1}\left(\frac{q(V+IR_S)}{e^{n_1KT}}-1\right)-I_{D2}\left(\frac{q(V+IR_S)}{e^{n_2KT}}-\frac{V+IR_s}{R_{sh}}\right) \quad (1)$$

Where I=Output current (A), V=Terminal voltage I_{ph}= photogenerated current (A), I_{01}=Saturated current of first diode I_{02}=Saturated current of second diode, n_1=ideality factor of first diode, n_2=ideality factor of second diode q=electronic charge, k= Boltzmann's constant and T= absolute temperature (K), R_{sh}=Shunt resistance and R_S=series resistance The open circuit voltage (Voc) is given by equation (2)

$$V_{oc}=\frac{KT}{q}\ln\left(\frac{I_{ph}}{I_{01}+I_{02}}+1\right) \quad (2)$$

where, V_{oc} is the open circuit voltage, I_{01} is the saturated current of first diode I_{02} is the saturated current of second diode, I_{ph} is the photogenerated current, q is the electronic charge, K is the Boltzmann's constant.

The fill factor FF is a measure of the ratio of maximum power output and the product of open circuit voltage and current density given by equation (3)

$$FF=\frac{P_{max}}{V_{oc}I_{sc}} \quad (3)$$

FF is the fill factor Pmax is the maximum power output, Voc is the open circuit voltage Jsc is the short circuit current density

$$PCE\ (\eta)=\frac{P_{max}}{P_{in}}=\frac{V_mI_m}{P_{in}} \quad (4)$$

$$PCE\ (\eta)=\frac{V_{oc}J_{sc}\times FF}{P_{in}} \quad (5)$$

η is the power conversion efficiency, P_{max} is the maximum power output, P_{in} is the power of the incident light on the solar cell V_m is the maximum voltage point and I_m is the maximum Current point.

MATERIALS AND METHODS

In this study, numerical simulations were conducted to evaluate and enhance the performance of $CuAlO_2$/ZnO and NiO/ZnO-based perovskite solar cells (PSCs). The investigation was aimed to optimize device efficiency by systematically varying critical physical and electrical parameters including layer thicknesses, operating temperature and their effects on electrical properties. The simulation was performed using SCAPS -1D (Solar Cell Capacitance Simulator), A one-dimensional solar cell modelling software version 3.3.10 fig 6 designed by the Department of Electronics and Information Systems (ELIS) at the University of Gent, Belgium (Pauwels and Vahoutte, 2007), The software is widely used for analysis of heterojunction-based devices, it can numerically fabricate solar cells by adding up to seven layers and is based on semiconducting equations including Poisson's and continuity equations (Marlein and Burgelman 2007). Graphs for I-V characteristics open circuit voltage (Voc), short circuit current density (Jsc), fill factor (FF), and Performance conversion Efficiency (PCE) were provided. The device architecture was investigated by stacking the hole transport layers ($CuAlO_2$ or NiO), absorber layer (Perovskite), electron transport layer (ZnO), and appropriate electrodes ITO and Ag. The working temperature was varied in the range 300K-400K in the interval of 20K each at constant thicknesses. The thicknesses of the individual layers of $CuAlO_2$, NiO and ZnO were varied in the range of 50 to 140nm in the interval of 10nm each while keeping the working temperature constant. Illumination source AM1.5G spectrum with an intensity of 1000w/m^2 was used to simulate standard sunlight. External vias voltage sweep (from 0Vto open circuit voltage Voc) Variation of temperature (300 to 400K), Series and shunt resistances incorperated to model practical loses. Figs. 2 and 4 show the structure of the PSC, which consisted of a front contact (ITO) an ETL (ZnO), the absorber (Perovskite), a HTLs ($CuAlO_2$), and (NiO) a back contact (Ag). This was the initial structure for PSC simulation. The simulation was performed using SCAPS-1D. in a photoelectric cell, such as the short circuit current (SC), when photons from sunlight strike the cell, electrons are generated and collected at the front contact (ITO) through the ETL. The photogenerated holes are collected at the back contact through the HTL. This process generates an electric current. The collection of electrons and holes at the front and back contacts, respectively, gave rise to a potential difference across the device. This potential difference is responsible for generating an electrical current in the device. All simulations were run at temperature range of 300-400K with 100 mW/ cm^2 illumination and an AM 1.5 G light spectrum. The capture cross sections for electrons and holes were fixed at 10^{15} cm^2. The initial parameters were as follows: Jsc = 12.743197 mA/cm^2, Voc = 1.4889 V, FF = 76.42%, and PCE = 14.50%.

Table 1: Input Parameters

Parameters	$CuAlO_2$	NiO	ZnO	Perovskite
Thickness (nm)	50	50	50	
	60	60	60	
	70	70	70	
	80	80	80	320
	90	90	90	
	100	100	100	
	110	110	110	
	120	120	120	
	130	130	130	
	140	140	140	
Bandgap Energy (ev)	3.5	3.7	3.3	1.55
Electron affinity χ (ev)	2	1.80	3.30	3.90
Relative permittivity ε_r	10	11	9	24
CB effective density of states Nc (cm^{-3})	2,0 X 10^{18}	2,0 X 10^{18}	2.2 X 10^{18}	1.0 X 10^{18}
VB effective density of states N_V (cm^{-3})	2.0 X10^{19}	2.0 X 10^{19}	1.8 X 10^{19}	1.0 X 10^{18}
Electron mobility μ_e (cm^2/V.s)	1.0 X -3	1 X 10^{-3}	20	10
Hole mobility μ_h (cm^2/V.s)	1. 0 X 10^{-1}	1.0	1 X 10^{-3}	10
Donor density N_D (cm^{-3})	1.0 X 10^7	1 X 10^7	1.0 X 10^{18}	1.5 X 10^{16}
Acceptor density N_A (cm^{-3})	1.0 X10^{19}	1.5 X 10^{16}	1.0 X 10^5	0

Defect density N_1 (cm^{-3})	1 X 10^{15}	1 X 10^{16}	1.0 x10^{14}	1 X 10^{15}

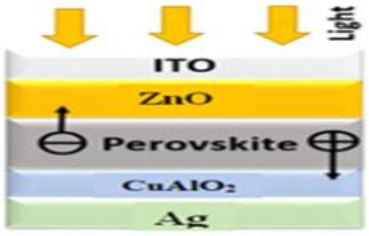

Figure 2: ITO, ZnO, ,Perovskite, $CuAlO_2$, Ag Device Structure

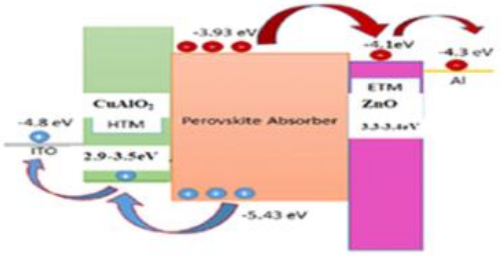

Figure 3: Schematic of Device Energy Level Diagram

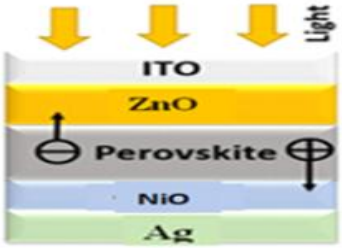

Figure 4: ITO, ZnO, Perovskite, NiO, Ag Device Structure

Figure 5: Schematic of Device Energy Level Diagram

Scaps-1dsimulationsoftware

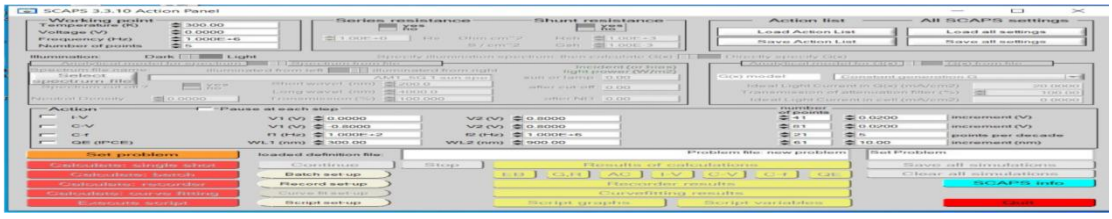

Figure 6: SCAPS1D3.3.10

RESULTS AND DISCUSSION

This chapter presents and discusses the results obtained from the numerical simulation of $CuAlO_2$/ZnO and NiO/ZnO perovskite solar cells using SCAPS-1D software. The simulations were carried out to evaluate and optimize the performance of these cells under varying physical and environmental conditions. Specifically, the study examined the effects of temperature variations and absorber layer thicknesses on the key photovoltaic parameters including i-v characteristics, open circuit voltage (Voc), Short circuit current (Jsc), fill factor (FF) and power conversion efficiency (PCE). The results were interpreted in the context of carrier transport mechanisms, recombination loses, and interface behaviour within the device structure.

Fig 7a shows a current density-voltage (J-V) characteristics of the $CuAlO_2$/ZnO perovskite solar cell across the temperature sweep of 300-400k with 40k interval, the device exhibits a decline in Voc from 1.05 to 0.95V and a slight rise in Jsc from 23-25mA/cm^2, FF drop from 77-66% leading to a net reduction in PCE from 18.6-15.7% these variations follow the expected thermal behavior aligns with the Shockley-Queisser model were elevated temperature increases recombination and series resistance loses, thereby reducing both Voc and FF despite modest gain in carrier generation, the curve at 300k demonstrates the strongest diode quality and highest performance, while the 400k curve reflects the onset of increased recombination and mobility limitations. Similar to the results obtained by (Chen *et al*., 2016 and Jeng *et al*., 2013).

Fig. 7b. shows a replicated temperature-dependent J-V curves for the NiO/ZnO perovskite solar cell at temperature sweep of 300-400k, values follow the same thermal trend as that of fig. 7a. with Voc decreasing from 1.02-0.09V while Jsc moderately increasing from 22.524.3mA/cm^2, FF drops from 77-66% and the corresponding PCE reduces from 17.7-15.3%. The replicated dataset confirms the stability and reproducibility of the simulation, consistent with typical perovskite temperature-dependence reported in literature by (Tress, 2017 and Chen, 2016). The monotonic decrease in Voc and FF with rising temperature follows the exponential increase in saturation current J_0 at high temperature accelerates recombination and lowers device efficiency (Shockley and Queisser 1961; Green, 1982). The voltage drop is traced to the temperature-induced increase of the diode saturation current and interface recombination in the perovskite/oxide contacts, therefore the I-V knee becomes more rounded and the maximum-power rectangle shrinks giving a lower PCE at 400k than at 300k. This agrees with the general temperature-dependence studies of perovskite and oxide solar cells, which reported that efficiency loss at high temperature is dominated by Voc and FF and not by Jsc (Mortadi, *et al.,*2025).

Fig.7c presents the I-V Characteristics of $CuAlO_2$-based perovskite solar cell at an initial temperature of 300k for varying HTL thicknesses of 50, 90 and 140nm. The simulated

results gave a numerical values revealing a strong thickness-dependent behavior at 50nm the reduced thickness results in lower Voc, Jsc and FF of 1.00V, 22.0mA/cm^2, 74% respectively due to insufficient optical absorption and reduced charge-collection efficiency. Increasing the thickness to 90nm significantly enhances performance giving the optimum value of Voc, Jsc, and FF of 1.06V, 24.0mA/cm^2 and 78% respectively, indicating an optimal trade-off between absorption, carrier transport and reduced recombination loses. Beyond the optimal point, at 140nm performance begun to decline because thicker $CuAlO_2$ increases series resistance and recombination before carrier extraction in agreement with the findings of (Ozgur, *et al*., 2005; Chen, 2016).

Fig.7d displays the I-V Characteristics of NiO-based perovskite solar cell at an initial temperature of 300k for varying HTL thicknesses of 50, 90 and 140nm. The simulated results as follows at 50nm the reduced thickness results in lower Voc, Jsc and FF of 0.99V, 22.0mA/cm^2, 74% respectively due to insufficient optical absorption and reduced chargecollection efficiency. Increasing the thickness to 90nm significantly enhances performance giving the optimum value of Voc, Jsc, and FF of 1.06V, 24.0mA/cm^2 and 77% respectively, indicating an optimal trade-off between absorption, carrier transport and reduced recombination loses. Beyond the optimal point, at 140nm performance begun to decline Voc, Jsc and FF drop to 0.95V, 22.3mA/cm^2 and 75% respectively, also consistent with the NiO's known tendency to accumulate defects and increase series resistance when too thick similar to the findings in the work of (Jeon, *et al*., 2014). Excessive thicknesses contribute to heightened trap-assisted recombination and reduced electric-field strength across the HTL. These trends follow established theoretical expectations for transition-metal-oxide transport layers by (Tumen *et al*., 2020). Since PCE depends entirely on Voc, Jsc and FF similar to equation 6 PCE increases from 16.12% at 50nm to 19.18% at 90nm and finally declined to 15.89%. At 140nm mainly due to increased series resistance, a longer carrier transport path and higher trap assisted recombination typical of thicker NiO films similar to the findings of (Jeon *et al*.,2014). Thus 90nm is the optimal NiO thickness for peak device efficiency at 300k.

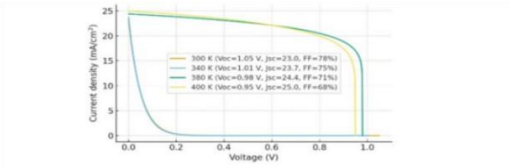

Fig 7a I-V curves for $CuAlO_2$/ZnO perovskite at 300K, 340k 380 a00k temperatures

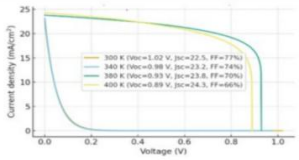

Fig 7b I-V curves for $CuAlO_2$/ZnO perovskite at 300K, 340k 380 a00k temperatures

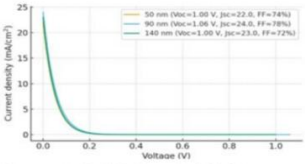

Fig 7c I-V curves for $CuAlO_2$ layer for initial temperature (300k) at layer thicknesses of 50, 90, and 140nm

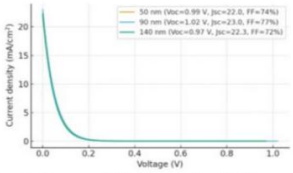

Fig 7d I-V curves for NiO layer for initial temperature (300k) at layer thicknesses of 50, 90, and 140nm

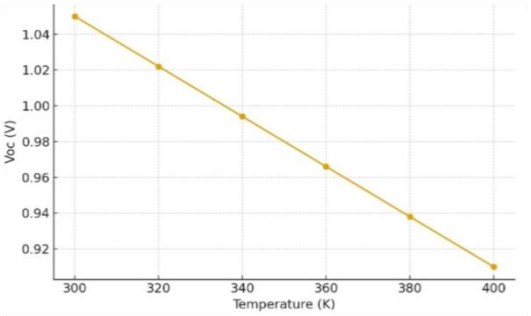

8(a)

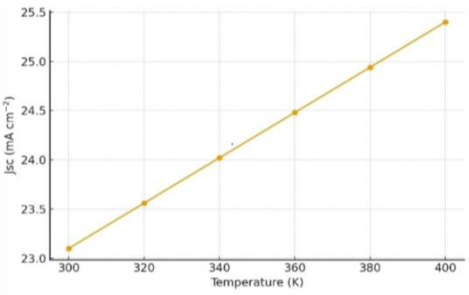

8(b)

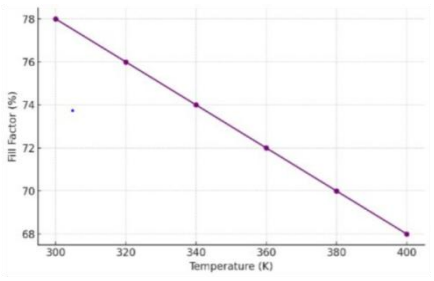

8(c)

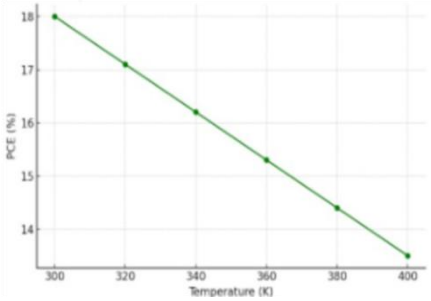

8(d)

Figure 8a-d: Effect of Variation in Performance Parameters with Increase in Temperature 300-400K of $CuAlO_2$/ZnO Perovskite Solar Cell

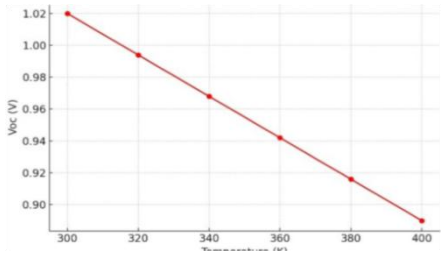

(8e)

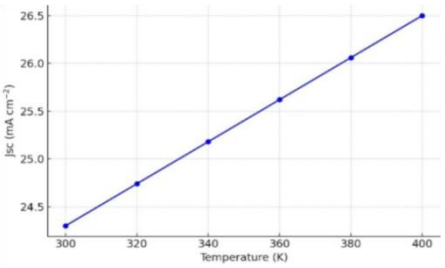

(8f)

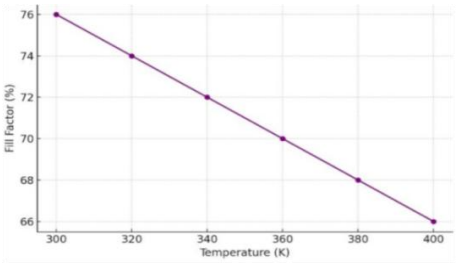

(8g)

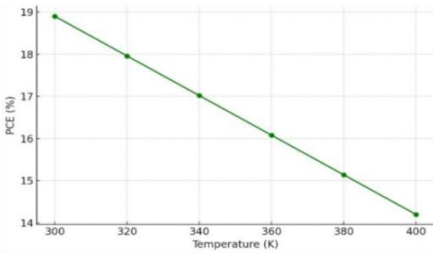

(8h)

Figure 8e-h: Effect of Variation in Performance Parameters with Increase in Temperature 300-400K NiO/ZnO Perovskite Solar Cell

Fig.8a-d shows the effect of rise in temperature from 300-400K, for $CuAlO_2$/ZnO stack where fig.9a showed a decrease in Voc (1.05-0.95V) because the diode saturation current J_0 grows exponentially with T which lowers Voc according to equation (2), Fig 8b shows a slight increase in Jsc (23-25mA/cm^2) showing weakly positive temperature due to enhanced carrier collection and minor band-gap narrowing at higher temperature this effects are consistent with many PCS reports one of which is by (Mortadi, *et al.,*2005). Fig.8c shows the decline in FF (78-68%) this is connected with equation (3) linking directly to Pmax, Voc and Jsc, indicating FF decreases with temperature because Pmax reduces faster than the product Voc.Jsc due to enhanced recombination and resistive loses where Voc and Jsc defines the theoretical rectangular area of the solar cell and Pmax defines the usable area (knee of the IV curve) these results is in agreement with that of (Tress, *et al*., 2012). Fig.8d PCE consequently falls (18-13.5%) since efficiency (ŋ) is proportional to the products of Voc, Jsc and FF and the reduction in Voc and FF dominate over the small Jsc gain there for PCE with temperature increase matches photovoltaic theory and temperature coefficient analysis for PCS also similar to the findings of (Sing, and Ravindra, 2012). While Fig.8e-h shows the effect of rise in temperature from 300-400K, for NiO/ZnO stack where, fig, 8e shows how Voc reduces from 1.02 at 300k to 0.087 at 400k while fig.8f Jsc slightly increases from 24.3 to 25.5 mA/cm^2, and in fig. 8g FF declines from 76.2% at 300k to 67.8% at 400k leading to corresponding reduction in PCE from 18.9% to 15.3%, of fig.8h, these results are also in agreement with the findings of (Sing, 2012). While ZnO (ETL) remains a favourable high mobility thermally robust contact but interfacial recombination at the perovskite/ETL boundary still grows with temperature this causes Voc and FF loses, this is in agreement with the findings of (Boryssiewicz, 2019).

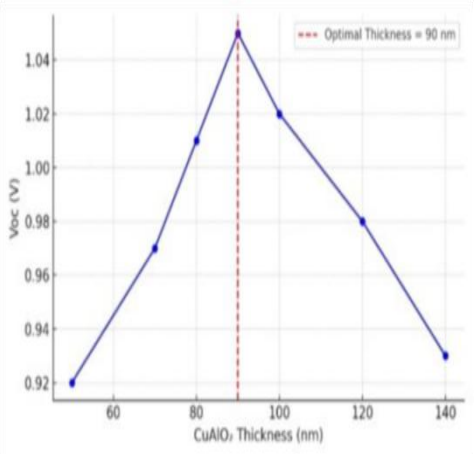

(9a)

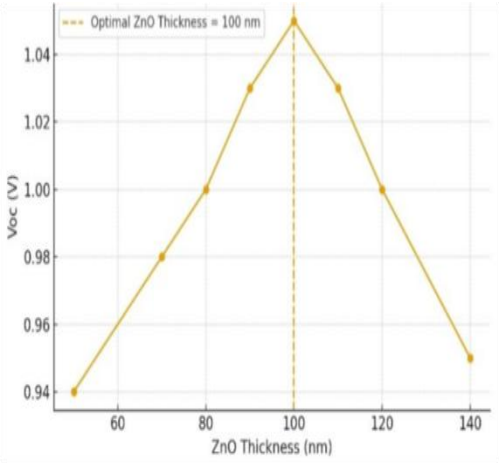

(9b)

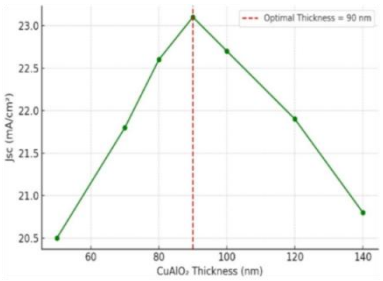

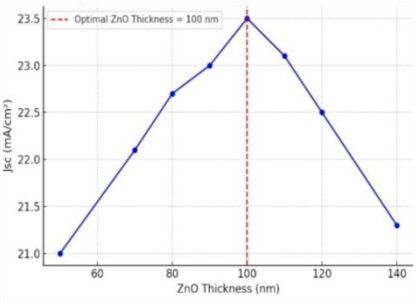

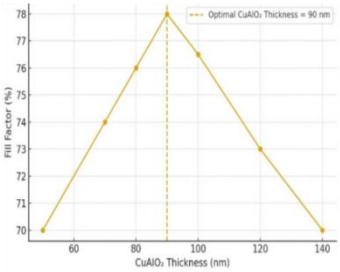

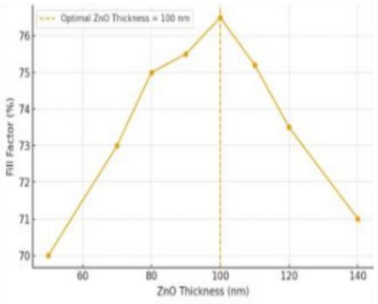

(9e) (9f)

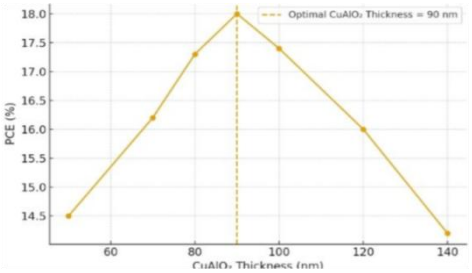

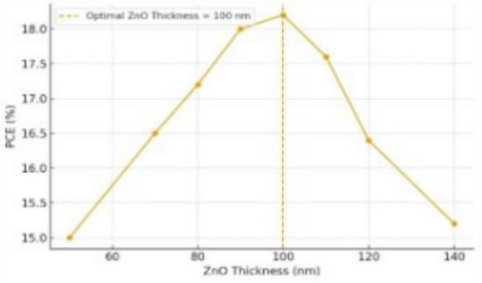

(9g) (9h)

Figure 9a-9h: Effects of Layer Thickness Variation of the Performance Parameters of $CuAlO_2$ and ZnO in perovskite Solar Cell

Figures 9a-h represent the I-V characteristics of plots for Voc, Jsc, FF and PCE as the layer thickness of $CuAlO_2$ and ZnO were varied from 50-140nm the results gave a trade-off between enhanced interfacial quality at moderate thickness, resistive and optical loses at higher thickness. In figs.9a and 9b $CuAlO_2$/ZnO PCS, optimal thickness of $CuAlO_2$ and ZnO were attained at 90nm and 100nm respectively at which Voc rises from 1.05V and reflecting reduced interfacial recombination as coverage improved, At lager thicknesses above (90100nm) Voc declined slightly because thicker layers reduces interface recombination and too thick add losses due to resistive limitations, this result is in agreement with the findings of (Rombach, *et al*., 2021). In fig.9c and 9d Jsc rose steadily to~ 23mA/cm^2 near 90nm $CuAlO_2$ and~ 100nm ZnO then saturated as parasitic absorption, trimming carrier collection and transport losses accumulated also in agreement with the results in the findings of (Alzoubi, *et al*., 2024). In figs.9e and 9f and FF peaked around the same thicknesses of 90nm and 100nm for $CuAlO_2$ and ZnO respectively before dropping with increased in series resistance this reflects the link the strong link between FF and series resistance as previously reported in transport layer optimization by (Green, 1982). In figs.9g and 9h, PCE reached~18% for both thicknesses at 90 and 100nm for $CuAlO_2$ and ZnO representing the optimal compromise between carrier and collection and transport resistance this are consistent with earlier study showing that optimized HTL/ETL thickness degrades conductivity and transparency by (Shockley, and Queiser, 961).

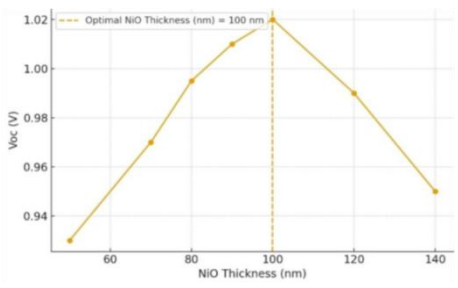

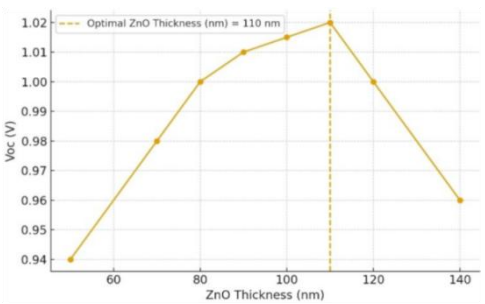

10a 10b

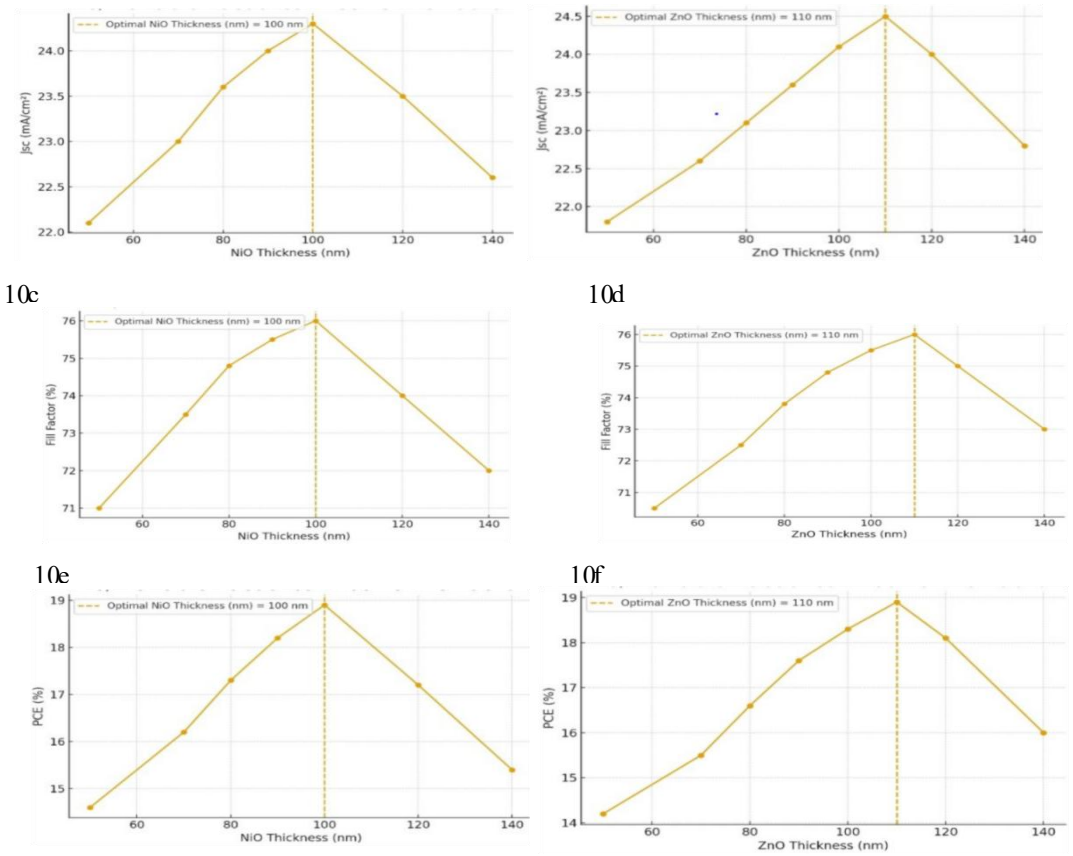

10c 10d

10e 10f

(10g) (10h)

Figure 10a-10h: Effects of Layer Thickness Variation of the Performance Parameters of $CuAlO_2$ and ZnO in Perovskite Solar Cell

Figures 10a-g represent the I-V characteristics of plots for Voc, Jsc, FF and PCE as the layer thickness of NiO and ZnO were varied from 50-140nm. In figs. 10a and 10b Voc improves and reaches optimum of~1.02 at the thicknesses of NiO and ZnO 100 and 110nm respectively and excess thickness raises resistive losses this result is in the same trend with that of the findings of (Rombach, *et al*., 2024). In figs.10c and 10d, Jsc increases to 24.3aA/cm^2 near 100nm NiO and 110nm ZnO driven by improved optical distribution and reduced pinholes, but declined at higher thickness due to resistive and optical losses also similar to the results of (Alzoubi, *et al*., 2024). In figs. 10e and 10f, FF is highly sensitive to thickness and reached an optimum value of 76% for NiO thickness 100nm and 110nm for ZnO decreasing thereafter due to effect of increase in series resistance accordingly, this also reflects the strong link between FF and series resistance, similar result was previously reported by (Green, 2016). Figs. 10g and 10h shows the variation of PCE with NiO and ZnO thicknesses, the device reached an optimum PCE of 18.9% at 100 and 110nm thicknesses respectively, and this is reflecting the combine influence of Voc, Jsc and FF as in equations (5) a theoretical context set by (Shockley and Queisser 1961). In line with this, the PCE aligns with the joint optimum of transport and optics. Also, in agreement with the findings of (Green, 2016).

CONCLUSION

In this work, the performance of perovskite solar cells based on $CuAlO_2$/ZnO and NiO/ZnO heterojunction architectures was investigated through numerical simulation using SCAPS-1D software. The simulation methodology involved varying both temperature (300–400 K, in 20 K intervals) and transport-layer thicknesses (50–140 nm, in 10 nm steps) to analyze the photovoltaic output parameters, including, I-V characteristics open-circuit voltage (Voc), short-circuit current density (Jsc), fill factor (FF), and power conversion efficiency (PCE). The results demonstrated that temperature rise leads to a gradual decrease in Voc (from ~1.05 to ~0.95 V for $CuAlO_2$/ZnO, and ~1.02 to ~0.89 V for NiO/ZnO between 300–400 K), accompanied by a modest increase in Jsc (23 - 25 mA/cm²), while FF declined (78 - 68%) and PCE decreased significantly (from 18% to ~13–14%). This behaviour reflects enhanced recombination and resistive losses at elevated temperatures, consistent with established perovskite device physics. For layer thickness variation, both $CuAlO_2$ and NiO (HTLs) and ZnO (ETL) exhibited clear optima in the 90–100 nm (HTL) and 100–110 nm (ZnO) ranges. At these thicknesses, the devices reached maximum performance, $CuAlO_2$/ZnO: Voc ≈ 1.05 V, Jsc ≈ 23 mA/cm², FF ≈ 78%, PCE ≈ 18% NiO/ZnO: Voc ≈ 1.02 V, Jsc ≈ 24.3 mA/cm², FF ≈ 76%, PCE≈18.9%. Although $CuAlO_2$ exhibited a slightly higher Voc, and FF, but NiO configuration demonstrates a higher PCE (18.9% vs 18%), making it more recommended in terms of practical performance efficiency. results confirm that optimal charge extraction and minimized recombination/series resistance are achieved at intermediate transport-layer thicknesses, whereas very thin layers suffer from incomplete coverage and very thick layers from increased resistance and parasitic absorption. Overall, the study validates SCAPS-1D as a powerful numerical tool for optimizing perovskite solar cell structures and provides quantitative evidence that both temperature management and precise HTL/ETL thickness control are crucial for enhancing device efficiency.

REFERENCES

Abdelrazek, A. S., Shaker, A., and Elgendy, H. (2021). Numerical modelling of perovskite solar cells using SCAPS-1D: A review. Renewable and Sustainable Energy Reviews, 147, 111240. 137(27), 8696–8699.

Abdoulsaad, M., El-Tahan, M. and Ebrahim, S. (2019). Thermal oxidation of sputtered nickel nano-film as hole transport layer for high performance perovskite solar cells. Open access vol.30, pages 19792-19803, (2019). Materials in electronics https://doi.org/10.1007/s10854-019-02345-2

Alzoubi. T., Kadhem, W. J., Gharram, M. A., Makhadme, G., Abdelfattah, M. A. O.,Abuelsamen, A., Al-Diabat, A. M., Noqta, O. A., Lazarevic, B., Zyoud, S. M. and Mourched, B (2024). Advanced Optoelectronic Modelling and Optimization of HTL Free $FASnI_3$/C60 perovskite solar cell Architecture for Superior performance. 2024.14(12):1062 doi: https://doi.org/10:3390/nano14121062

Ahn, N., Son, D. Y., Jang, I. H., Kang, S. M., Choi, M., & Park, N. G. (2015). Highly reproducible perovskite solar cells with average efficiency of 18.3% and best efficiency of 19.7% fabricated via Lewis base adduct of lead (II) iodide. Journal of the American Chemical Society,

Bouich, A., El Kenz, A., Lanaya, K., Oulmi, Y., El Madani, A., & Choukri, A. (2023). Delafossite as hole transport layer: A new pathway for inorganic lead-halide perovskite solar cells. Solar Energy, 250, 58–69. https://doi.org/10.1016/j.solener.2023.01.022

Boryslewicz, M. A. (2019) ZnO as a Functional Material, a review Ai Lotrikow 32/46,02-668 Warsaw-Poland-https://doi.org/10.1016/3390/crystal9100505

Burgelman, M.,Verschraegen, J., Degrave, S., & Nollet, P. (2013). Advanced electrical simulation of thin film solar cells. Thin Solid Films, 535, 296–301. https://doi.org/10.1016/j.tsf.2012.12.032

Chang, T. C., Huang, Y. J., Lin, C. H., Chen, C.-W., & Chiu, C. H. (2023). Investigation of the performance of perovskite solar cells with ZnO interlayers. Nanomaterials, 13(9), 2202. https://doi.org/10.3390/nano13092202

Chen, W., Wu, Y., Liu, J., Qin, C., Yang, X., Islam, A., Cheng, Y., and Han, L. (2013). Hybrid interfacial layer Leads to solid performance Improvement of Inverted perovskite Solar Cells DOI: https://doi.org/10.1039/c0ca00000s

Chowdhury, T. H., Ahmed, S., & Chowdhury, M. S. (2020). Impact of temperature on perovskite solar cell performance: A simulation study. Solar Energy, 203, 332–339.

Dupré, O., Vaillon, R., & Green, M. A. (2015). Physics of the temperature coefficients of solar cells. Progress in Photovoltaics: Research and Applications, 23(12), 1847–1858. https://doi.org/10.1002/pip.2596

El-Ahmar, M., Abou-Hashema. A., and Ashraf, M. M. (2016). Mathematical modelling of Photovoltaic module and evaluating the effect of various parameters on its performance DOI:-10.1109/MEPCON.2016.7836976

Fleischer, K.. Norton, E., Mullakey, D., Caffrey, D. and Shvets, I. (2017). Quantifying the Performance of p-Type Transparent Conducting Oxides by Experimental Methods. Materials (basel).2017 Sep 1;10(9):1019. Doi: https://doi.org/10.3390/ma10091019

Islam, M. B., Yanagida, M., Shirai, Y., Nabetani, Y. and Miyano, M. (2017). NiO_x Hole Transport layer with improved Stability and Reproducibility. ACS Omega.2017 May 24;2(5):2291-2299. doi: https://doi.org/101021/acsomega.7b00538

Kojima, A., Teshima, K., Shirai, Y., & Miyasaka, T. (2009). Organometal halide perovskites as visible-light sensitizers for photovoltaic cells. Journal of the American Chemical Society, 131(17), 6050–6051.

Green, A. M. (1982). Accuracy of analytical expressions for solar cell fill factors s c i e n c e Directvol.7-issue-3-pages-337-230-https://doi.org/10.1016/0379- 6787(82)90057-6

Green, M. (2016). Accurate expressions for solar sell fill factor including series and shunt resistances,-Appl.phys.Lett.108,081111(2016).-https://doi.org/101063/1.4942660

Gulomova, I., Accouche, O., Aliev, R.., Al Barakeh, Z. and Aduazimov, V. (2024). Optimization Geometry and ETL Materials for High-Performance Inverted Perovskite Solar Cells Simulation, PMC11313813, doi: https://doi.org/103390/nano14151301

Hossain, K. M., Ishraque, G. F. and Mushtaq, M. (2023). An extensive study on multiple ETL and HTL Layers to design and simulation of high-performance lead-free $CsSnCl_3$based perovskite solar cells (2023).-Scientific-reports-13,-Article-number-2521 doi:org/10:1038/s41598-023-28506-2

Jeng, J., Chiang, Y. F., Lee, M. H., Peng, S. R., Guo, T. F., Chen, P. and Wen, T. C. (2013). $CH_3NH_3PBI_3$ Perovskite/Fullerence planar-Heterojunction Hybrid solar cells Advanced materials 2013, 25 (27) 3727-3732. DOI: https://doi.org/10.1002/adma.201301327

Jeon, N.J., Noh, J. Y., Yang, W. S., Kim, Y. C., Ryu, S. and Seok, S. I. (2014) Compositional engineering of perovskites for high-performance solar cells Nature, 517, 476-480

Mahmood, K., Sarwar, S., & Mehran, M. T. (2017). Current status of electron transport layers in perovskite solar cells: Materials and properties. RSC Advances, 7(28), 17044–17062. https://doi.org/10.1039/C6RA28988F

Mann, D. S., Singh, H., Gupta, S., Arora, R., & Mehta, N. (2024). Interfacial engineering of the nickel oxide–perovskite interface for inverted perovskite solar cells. Small, 20(12), 2405953.-https://doi.org/10.1002/smll.202405953

Marlein, J. Burgelman M. (2007) Proceedings of NUMOS (Int. Workshop on Numerical Modelling of Thin Film Solar Cells, Gent (B), 28-30 March 2007). p. 227-233 2007.

Mohammadian, H., Sarcheshmeh, M. and Ardakani, M. (2018). Recent advancements in compact layer development for perovskite solar cells. Volume 4 issue 11 November 2018, https//:doi.org/10.1016/j.heliyon.2018.e00912

Mortadi, A. Tabbai, Y., Elhafidi, E., Nasrellah, H., Chahid, E., Monkade, M., and Elmoznine, R. (2025) Investigating temperature effects on perovskite solar cell performance via S C A P S - 1 D - a n d - i m p e d a n c - s p e c t r o s c o p y - S c i e n c e D i r e c t https://doi.org/10.1016/j.clet.2024.100876

Navas, J., Sánchez-Coronilla, A., Gallardo, J. J., et al. (2018). ZnO/NiO nanostructures as efficient electron/hole transport layers for perovskite solar cells. Scientific Reports, 8(1), 1–12.

Ozgur, U., Alivoy, Y. I., Liu, C., Teke, A., Reshchiko, M. A., and Avrutin, V. (2005). A comprehensive review of ZnO materials and devices. Journal of Applied physics 98(4), 041301

Pauwels, H.J. Vanhoutte, G. (2007) Influence of interface states and energy barriers on efficiency of heterojunction solar-cells, J. Phys. D-Appl. Phys., 11 649-667.

Rombach, F M., Haque, S. A. and Macdonald, T. H (2021). Lesson learned from spiroOMeTAD and PTAA in perovskite solar cell. Energy Environ. Sci. 2021.14.51615190 DOI:10.1039/DIEE02095A (Review Article)

Sarkar, D. K., Mandal, S., Hossain, S. S., and Banerjee, S. (2024). Numerical investigation of green-synthesized $CuAlO_2$ as an HTL in Pb-free perovskite solar cells Heliyon,10, e2300856.- https://doi.org/10.1016/j.heliyon.2024.e2300856

Savva, A., Papadas, I. T., Tsikritzis, D., Ioakeimidis, A., Galatopoulus, F., Kapnisis, K., Fuhrer, R., Hartmeier, B., Oszajka, M. F., Kennou, S., and Choulis, S. A. (2019). Inverted perovskite photovoltaic using flame spray pyrolysis solution based $CuAlO_2$/CuO Hole selective contact ACS Appl Energy Mater.2019. 25;2(3):22762287 doi: https://doi.org/10.1021/acsaem.9b00070

Sing, P. Ravindra, N.M. (2012) Temperature dependence of solar cell performance-an analysis. ELSEVIER, Solar energy materials and solar cell 101 36 45

Shockley, W. and Queisser, H. J. (1961). Detailed balance limit of p-n junction solar cells. Journal of Applied Physics 32(3), 510-519. https://doi.org10.1063/1.1736034

Tress, W., Yavari, M., Dominski, K., Yadav, P., Niesen, B., Correra, J. P., Hagfeldt. A. and Graetzel. M.(2018) Interpretation and evolution of open-circuitvoltage, recombination, ideality factor and subgap defect states during reversible light-soaking and irreversible degradation of perovskite sola cells. Energy and Environment.

Tress, W. (2017). Organic inorganic halide perovskite; Fundamentals of solar cells, stability and charge carrier dynamics.

Tumen-Ulzii, G., Matsushima, T., Klotz, D., Leyden, M. R., Wang, P., Qin, c., Lee, J., Yang, Y., and Adachi, C. (2020). Hysteresis-less and stable perovskite solar cells with a selfassembled monolayer communication material 1(1) https://doi.org/10.1038/s43246020-0028-z

Wang, T., Ding, D., Wang, X., Zeng, R., Liu, H., and Shen, W. (2018). High-Performance Inverted perovskite Solar Cells with Mesoporous NiOx Hole transport Layer by Electrochemical Deposition-(2018).-ACS-Omega-2018,-3,12,18434-18443 https//:doi.org/10:1021/acsomega.8b02612

Wu, X., Zhang, J., Chen, Y., Li, H., and Zhou, M. (2022). ZnO electron-transporting layer engineering-realized-over-wide-temperature-windows.EcoMat,-4e-12192. https://doi.org/10.1002/eom2.12192